Sub-critical crack growth based time-dependent deformation model and its application to open-pit slope stability

Tao Xu, Zhiguo Li, Tianhong Yang, Xiaobin Zheng, Wancheng Zhu
Center for Rock Instability & Seismicity Research, Northeastern University, Shenyang, China

Tengfei Fu
CSCEC-TAISEI Construction Ltd., Beijing, China

ABSTRACT: A subcritical crack growth based deformation model was established to describe the time-dependent deformation and fracturing of rock. In conjunction with the uniaxial compression test of rock, the microscopic parameters of the model were calibrated, and the accuracy of the creep model and parameter calibration were verified using uniaxial compressive creep tests. Finally, the established time-dependent deformation model of rock was applied to the time-dependent deformation analysis of a slope in the Fushun West open-pit mine. This study shows that the time-dependent deformation model of rock established in this study can effectively describe the accelerated stage of rock creep, and the simulation results agree well with the experimental results. After the continuous deformation, cracks are formed by the stress concentration at the bottom of the slope under the influence of unfavorable factors, which continuously extend to the top of the slope and form a sliding surface, resulting in unstable sliding.

Keywords: rock slope, creep deformation, subcritical crack growth, slope stability, numerical simulations.

1 INTRODUCTION

The time-dependent deformation of rock mass can lead to damage deformation or even destruction of engineering rock mass, and the time-dependent mechanical properties and long-term stability of engineering rock mass have been the focus. It was an effective way to study rock time-dependent deformation to establish a model of rock time-dependent deformation to analyze the behavior of rock deformation under different environments. It has been proved that the theory of subcritical crack propagation can explain the time-dependent deformation mechanism of rocks on the mesoscale (Atkinson BK, 1987; Michalske TA, 1982; Potyondy, 2007).

In this paper, the stress corrosion theory was introduced into the three-dimensional discrete element program 3DEC to establish the rock time-dependent deformation model based on the stress corrosion theory. Combined with the uniaxial compression test of rock, the microscopic parameters of the model were calibrated, and the accuracy of the creep model and parameter calibration were verified based on uniaxial compressive creep tests. Finally, the established time-dependent

deformation model of rock was applied to the time-dependent deformation analysis of the Fushun West open-pit mine.

2 SUBCRITICAL CRACK GROWTH BASED TIME-DEPENDENT DEFORMATION MODEL

2.1 Subcritical crack growth model

The relationship between the subcritical crack growth rate and the stress intensity factor in the stress corrosion process was given by(Charles, 1958a, 1958b)

$$v = v_0 \exp(-\Delta H/RT) K_{\mathrm{I}}^{n} \tag{1}$$

where v is the crack growth rate, v_0 is the pre-exponential factor, ΔH is the activation enthalpy, R is the universal gas constant, T is the absolute temperature, n is a material constant known as the stress corrosion index, and K_{I} is the stress intensity factor.

Based on the chemical reaction rate theory, it is further assumed that static fatigue of glass is the result of a chemical process initiated by stresses between the environment and the glass. The crack growth rate is proportional to the rate of chemical reaction at the crack tip. A quantitative rate equation describing the crack growth rate is given (Potyondy, 2007).

$$v = v_0 \exp\left(\frac{v^{+}\sigma - (E^{+} + v_M \gamma/\rho)}{RT}\right) \tag{2}$$

where v^{+} is the activation volume, σ is the crack-tip tensile stress, $E^{+}$is the stress-free activation energy, v_M is the molar volume of the glass, γ is the interfacial surface energy between the glass and the reaction products and ρ is the radius of curvature of the crack tip. This equation was not formulated in terms of fracture mechanics parameters, such as the stress intensity factor K_{I}.

2.2 Formulation of the time-dependent model

The mesoscopic numerical model of rock is established using Voronoi polyhedron discrete model. In the numerical model, each polyhedron consists of several triangular sub-contact. Stress corrosion refers to the phenomenon that the mechanical properties of rock deteriorate over time and eventually become unstable. Stress corrosion model is programmed into a three-dimensional discrete element model. The stress corrosion model and corrosion rate curve are shown in Figure 1. We assume that the stress corrosion reaction occurs only at the contact between grains, and that the tensile strength and cohesion of the interface decay at a uniform rate proportional to the rate of chemical reaction (Xu et al., 2020).

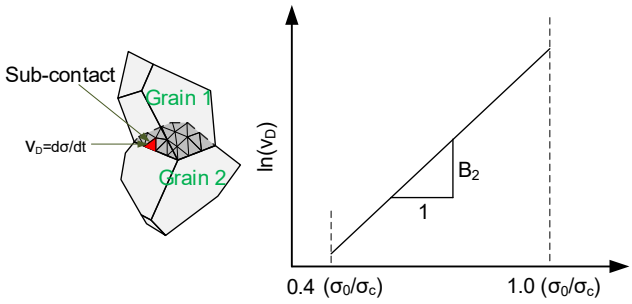

Figure 1. Degradation rate relations for the 3DEC-GBM. $\sigma_0$is the threshold stress below which stress corrosion does not occur, and σ_c is the peak strength.

When the temperature and humidity of the environment around the rock are constant, Equation 3-5 provides the degradation rate (v_D) of mechanical parameters at the interface:

$$v_D = \begin{cases} 0 & (\bar{\sigma} < \sigma_0) \\ B_1 e^{B_2 \bar{\sigma}} & (\sigma_0 \le \bar{\sigma} < \sigma_c) \\ \infty & (\bar{\sigma} > \sigma_c) \end{cases} \tag{3}$$

$$B_1 = \mathrm{A} v_0 e^{\left(-\left(E^+ + \frac{v_M \gamma}{\rho}\right)/RT\right)} \tag{4}$$

$$B_2 = v^+/RT \tag{5}$$

where σ_0 is the threshold stress (or so-called activation stress) below which stress corrosion reactions cannot occur (approximately equal to $0.4 * \sigma_c$)(Potyondy, 2007), $\sigma_c$is the peak strength, $\bar{\sigma}$ is the reaction-site stress at the sub-contact, and A is the constant of proportionality between the chemical reaction rate and the degradation rate.

3 MODEL VALIDATION

3.1 Uniaxial compression

In this study, sandstone was selected to verify the model. The average value of mineral mechanical parameters was used for particle parameters. For particle contact parameters, the mesoscopic parameters of particle contact were determined by trial-and-error method (Gao & Kang, 2017; Li, Li, & Zhao, 2017). The mesomechanical parameters of the final model are presented in Table 1. The experimental and creep curves obtained by us are shown in Figure 2, and the simulation curve is in good agreement with the experimental curve.

Table 1. The mesoscale physical properties used to study the mechanical behavior (found through calibration). E - Young's modulus; ν - Poisson's ratio; K_n -normal stiffness of the sub-contact; K_s -shear stiffness of the sub-contact; J_T -tensile strength of the sub-contact; J_c -cohesion of the sub-contact; φ -friction angle of the sub-contact; φ_r -residual friction angle of the sub-contact.

E/GPa	$K_n/GPa \cdot mm^{-1}$	ν	K_n/K_s	J_T/MPa	J_c/MPa	$\varphi/°$	$\varphi_r/°$
12	40	0.27	2	7.6	31.2	27	6

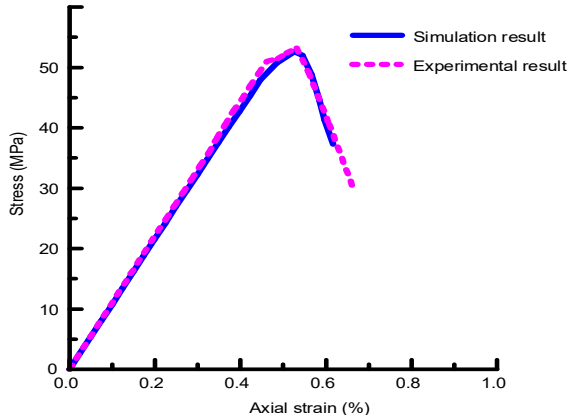

Figure 2. Uniaxial compression and numerical simulated curves.

3.2 Uniaxial compressive creep tests

The two parameters B_1 and B_2 are related to the environment of rocks. Here, the values could be determined by trial and error. First, the parameter sensitivity analysis of B_1 and B_2 was carried out to determine their influence on the creep behavior simulated by the model. Then, the available B_1 and B_2 were calibrated based on the uniaxial compression creep test curve. The calibrated subcritical crack growth parameters were B_1 =2.87×10^{-3} and B_2 =4.37×10^{-8}, respectively. Figure 3 shows the numerically simulated and the experimental creep curve of rock in uniaxial compression. It can be seen from Figure 3 that the simulated curve is in good agreement with the experimental curve, which verifies the accuracy of our established time-dependent deformation model.

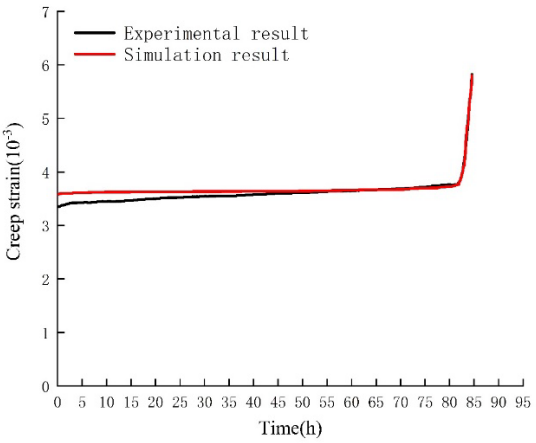

Figure 3. Comparison between numerically simulated and experimental curve in uniaxial creep tests.

4 CASE STUDY

4.1 Geological setting

The Fushun West open-pit mine, located in the city of Fushun in Liaoning in northeast China, is 6.6 km long, 2.2 km wide, and 418 m deep. It produces 4.5 million tons of coal and 12 million tons of oil shale annually. The inclination of the coal formation in the mine varies from 20° to 40°. The coal seam varies in depth from 40 m in the eastern section of the mine to 120 m in the west. Shales and mudstones with an average depth of 360 m, lie above the oil shale. A wedge-shaped landslide occurred on the E900 ~ E1200 northern bank of the mine in September 2014. The elevation of the back edge of the sliding body, the shear outlet of the front edge, and bottom of the shale are 80, 252, and 220 m below ground level, respectively.

4.2 Numerical model

We established a three-dimensional model of Fushun West open-pit mine, as shown in Figure 4. The 3D model of the chosen part of slope E1000 is 278 m in height, 625 m in length, and 370 m in width. According to the geological survey, there are two groups of obvious faults in the landslide area. The linear elastic model was used for Voronoi polyhedrons, and the Coulomb slip model was used for interfaces between layers and between Voronoi polyhedrons within layers. In addition, the left and right boundary areas of the slope model are not the same, therefore, the application of stress boundary on the left and right sides of the slope model will cause the boundary to suffer from unequal forces, and the model will rotate or move. The displacement boundary conditions of this model was adopted. The top surface of the slope model was set as a free surface, and the normal velocity of the surrounding boundary of the model was set as 0.

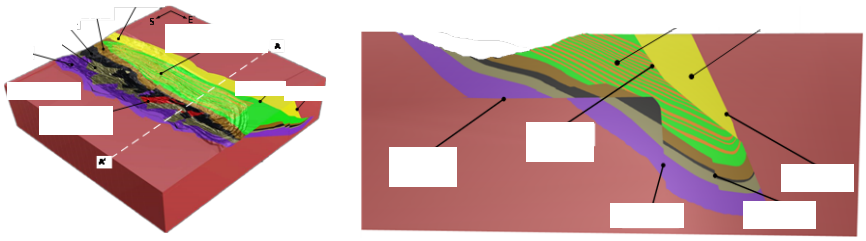

Figure 4. 3D geological model of Fushun West Open-pit Mine and A-A′ cross-section.

4.3 Model input parameters calibration

The dimensions of the established discrete Voronoi polyhedral models are 150 m × 5 m × 300 m (length × width × height) and 150 m × 5 m × 150 m (length × width × height) respectively. The top and bottom sides of the model are subjected to displacement loading to complete the compression simulation test. The top and bottom end faces of the model were loaded normally, and a horizontal displacement load was applied to the left half of the surface to complete the shear simulation test. Through a series of simulations and calibrations, the meso-mechanical parameters of the different rock layers of the slope model were determined (see Table 2).

Table 2. The calibrated physico-mechanical parameters on a meso-scale.

Lithology	E/GPa	ν	$K_n/GPa \cdot m^{-1}$	$K_s/GPa \cdot m^{-1}$	J_T/MPa	J_c/MPa	$\varphi/°$
Sandstone	3.4	0.20	60	10	1.80	6.30	27
Mudstone	1.5	0.28	8	1.4	1.70	0.35	27

4.4 Time-dependent deformation and instability of northern slope

In this study, the time step of stress corrosion and the smaller value of the time step calculated by dynamics are chosen as the time value of the model. Figure 5 shows the simulated aging deformation and instability process of the north side E1000 of Fushun West open-pit mine in 2014. In the simulation calculation, the slope continued its time-dependent deformation, resulting in stress concentration at the bottom of the slope and cracks that gradually expanded to the top of the slope. The time-dependent deformation of the slope could be divided into three phases. In the first phase, the lower part of the landslide slides significantly. Under the influence of the fault, the fracture area of the slope gradually shifts upward. In the second phase, sliding of the entire landslide occurs. The landslide slides about 45.9 m to the left (to the free side of the slope). The landslide continues to move towards the open side of the slope. In the third phase, the landslide slid about 79 m to the left (towards the open side of the slope).

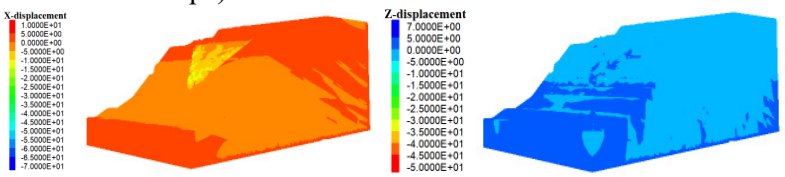

(a) In the first phase

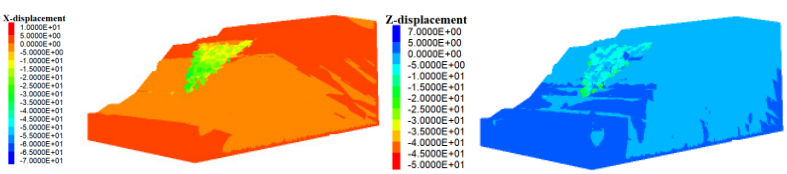

(b) In the second phase

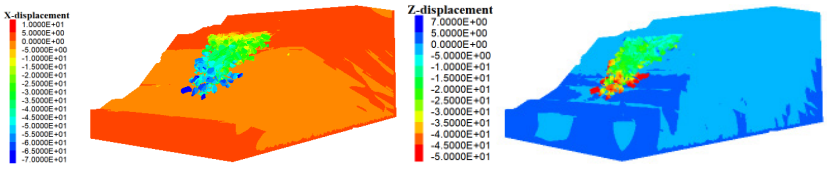

(b) In the third phase

Figure 5. The time-dependent displacement in the stability process of the north slope. Since the horizontal deformation of the slope is mainly the deformation along the slope inclination direction, the horizontal deformation here refers only to the deformation along the slope inclination direction. The downward and leftward displacement are negative values.

5 CONCLUSIONS

We introduced stress corrosion theory into the discrete block model, determined the mesoscopic parameters of the model by uniaxial compression experiment, and verified the effectiveness of the model by uniaxial compression creep experiments. We applied the established time-dependent deformation model of rock to the analysis of the stability of the north side slope of Fushun West open-pit mine. Under the influence of unfavorable factors, the stresses concentrate at the lower part of the slope and cracks appear, and the slope expands further into the upper part of the slope to form a sliding surface, and unstable sliding occurs. The time-dependent deformation instability process of profile E1000 determined by the simulation is close to the area of the landslide on site, which is consistent with the location and shapge of the landslide on site.

ACKNOWLEDGEMENTS

The work was jointly supported by NSFC (42172312, 51974062 and 52211540395).

REFERENCES

Atkinson BK, M. P. (1987). The theory of subcritical crack growth with applications to minerals and rocks. Fracture mechanics of rock. *Fracture mechanics of rock, 2*, 111-166.

Charles, R. J. (1958a). Static Fatigue of Glass. I. *Journal of Applied Physics, 29*(11), 1549-1553. doi:10.1063/1.1722991

Charles, R. J. (1958b). Static Fatigue of Glass. II. *Journal of Applied Physics, 29*(11), 1554-1560. doi:10.1063/1.1722992

Gao, F., & Kang, H. (2017). Grain-Based Discrete-Element Modeling Study on the Effects of Cementation on the Mechanical Behavior of Low-Porosity Brittle Rocks. *International Journal of Geomechanics, 17*(9). doi:10.1061/(asce)gm.1943-5622.0000957

Li, X. F., Li, H. B., & Zhao, J. (2017). 3D polycrystalline discrete element method (3PDEM) for simulation of crack initiation and propagation in granular rock. *Computers and Geotechnics, 90*, 96-112.

Michalske TA, F. S. (1982). A molecular interpretation of stress corrosion in silica. *Nature, 295*(5849), 511-512.

Potyondy, D. O. (2007). Simulating stress corrosion with a bonded-particle model for rock. *International Journal of Rock Mechanics and Mining Sciences, 44*(5), 677-691. doi:10.1016/j.ijrmms.2006.10.002

Xu, T., Fu, T. F., Heap, M. J., Meredith, P. G., Mitchell, T. M., & Baud, P. (2020). Mesoscopic Damage and Fracturing of Heterogeneous Brittle Rocks Based on Three-dimensional Polycrystalline Discrete Element Method. *Rock Mechanics and Rock Engineering, 53*(12), 5389-5409. doi:10.1007/s00603-020-02223-y